Magnetic Force Microscopy Revealing Long Range Molecule Impact on Magnetic Tunnel Junction Based Molecular Spintronics Devices

Pawan Tyagi[1,2] and Christopher Riso[1]

University of the District of Columbia, Department of Mechanical Engineering, 4200 Connecticut Avenue NW Washington DC-20008, USA[1]

Email: ptyagi@udc.edu*

University of Kentucky, Chemical and Materials Engineering Department, 177 F Paul Anderson Hall, Lexington, KY-40506, USA[2]

Abstract: Magnetic force microscopy (MFM) vividly showed that organometallic molecules, when bridged between two ferromagnetic electrodes along the cross-shaped magnetic tunnel junction edges transformed the magnetic electrodes itself. Molecules impacted a large area of ferromagnetic leads around the junction at room temperature and complement the previous magnetic measurements showing molecule effect on pillar form magnetic tunnel junctions [Ref. P. Tyagi et. al. Nanotechnology, 2015, Vol. 26, p 305602]. This molecule induced changes in the magnetic electrodes impacted the transport of the magnetic tunnel junction and stabilized as much as seven orders smaller current at room temperature. We have discussed the current suppression phenomenon in the recent publication [Ref. Tyagi et al., Organic Electronics, 2019, Vol. 64, p 188]; however, we did not provide any direct evidence of molecule impact on ferromagnetic electrodes around molecule junction. Our MFM studies in this paper suggests that molecule effect was observable several μm away from the molecule-metal junctions. Our study suggests that magnetic tunnel junction based molecular spintronics devices can be a gateway to a vast range of commercially viable and robust futuristic computer devices and highly correlated materials.

Key Words: Molecular spintronics; magnetic molecules; ferromagnets; magnetic tunnel junctions.

Introduction: Molecules are unequivocally the most configurable and mass producible nanostructures known to mankind[1]. Utilizing molecules in spin-based logic and memory devices may produce novel

forms of futuristic computer hardware[2]. However, to date, experimental molecular spintronics field has not been able to progress significantly due to the limitations of conventional device fabrication approaches[3]. Similar to the development of magnetic tunnel junction (MTJ) technology [4], advancement of molecular spintronics field critically depend on the ability to conduct insightful magnetic measurements. It has been shown that MTJ based molecular spintronics devices (MTJMSDs) can provide a robust method of integrating molecular device elements with ferromagnetic electrodes[5, 6] and address limitations of conventional approaches[7-10] . As discussed in a previous review papers[11], MTJMSDs can be a critical technology for (i) adding enormous potential to current MTJ technology[12, 13], and (ii) resurrecting the experimental research in molecular devices by addressing the limitations of the conventional approaches. A prefabricated MTJ (Fig. 1a), where the minimum gap between the top and bottom ferromagnetic electrodes is equal to the tunneling barrier, can allow the covalent bonding of different types of ferromagnetic films with desired molecules (Fig. 1b-c). Most importantly, the burden of mechanically separating the two ferromagnetic electrodes is borne by the insulating tunneling barrier (Fig. 1c). Hence, a molecule, covalently bonded to the ferromagnetic electrodes (Fig. 1c), get unprecedented opportunity to display their full potential as a spin channel. Under such unprecedented favorable state molecules can produce a very strong effect on overall magnetic and transport properties which are even evident at room temperature[6, 14, 15]. Several magnetic study methods such as SQUID magnetometer, ferromagnetic resonance, and magnetic force microscopy (MFM), have been applied on the large array of cylindrical MTJ pillars before and after transforming them into MTJMSDs[6]. These studies have given us tremendous insight into the impact of molecule induced strong coupling. However, the realization of molecular spintronics devices requires long ferromagnetic leads to connect molecule with the outer world. Unfortunately, all the magnetic measurements do not become applicable for the MTJMSD in the cross-junction form where ferromagnetic leads are much larger than the cross junction of ferromagnetic films where molecules are attached. MFM is very promising in studying the individual MTJMSD and

ferromagnetic leads. Here, we discuss the MFM and supporting studies to highlight the attributes of integrating paramagnetic molecules along the MTJ edges.

Experimental details: We have utilized previously demonstrated liftoff based MTJMSD fabrication approach[5, 11] to produce samples for the present study. These MTJMSDs are formed by covalently bridging the Octametallic Molecular Complexes (OMCs) between the top and bottom ferromagnetic electrodes of an MTJ (Fig. 1b-c). An OMC possessed cyanide-bridged Ni and Fe metal ions and $[(pzTp)Fe^{III}(CN)_3]_4[Ni^{II}(L)]_4[O_3SCF_3]_4$ [(pzTp) = tetra(pyrazol-1-yl)borate; L = 1-S(acetyl)tris(pyrazolyl)decane][16] chemical structure. In this study, the MTJ with Ta(5 nm)/Co(5-7 nm)/NiFe(5-3 nm)/AlOx(2 nm)/NiFe (10 nm) configuration was utilized. Utilizing cobalt (Co)

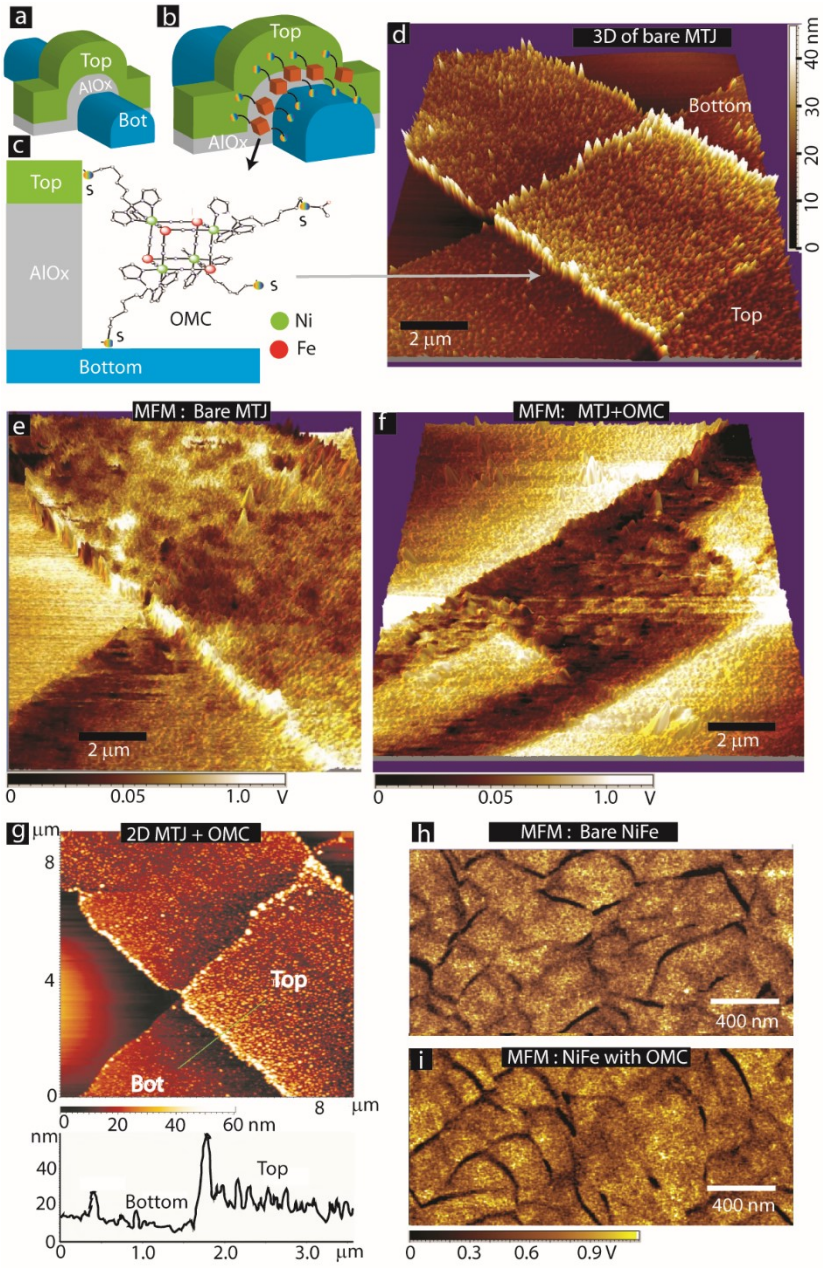

Fig. 1 Schematic of exposed edge tunnel junction (a) before and (b) after hosting OMC channels. (c) Magnified version of one molecule connected to the ferromagnetic electrodes via thiol groups. (d) 3D topographical image of an MTJ with 5µm x 5µm junction area. MFM color superimposed on topographical AFM image of MTJ (e) before and (f) after hosting OMC molecular channels along the exposed edges. (g) 2D topographical image of OMC treated MTJ showing MFM contrast disappearance along top electrode in (f). Cross sectional panel show the difference in top and bottom electrode. MFM of an unpatterned NiFe film (h) before (i) and after interaction with OMC.

in the bottom electrode increased the magnetic hardness of the ~5 μm wide bottom electrode as compared to 5-10 μm wide top NiFe electrode. Bottom electrode possessed four-fold wider hysteresis loop as compared to the top NiFe electrode [6]. An OMC possessed ten carbon long tethers terminated with the thiol bonds that helped make NiFe –OMC covalent bonding [16, 17]. Also, experimental details about MTJMSD fabrication[5], OMC attachment[5], OMC synthesis and characterization[17] has been published elsewhere. For the MFM studies, Molecular Imaging Pico-Scan atomic force microscope (AFM) and a Co coated Nanoscience Nanosensor brand magnetized cantilevers were utilized. MFM cantilevers were magnetized along the direction to the MFM tip using a permanent magnet. During MFM distance between magnetic cantilever and sample was 50-100 nm above the MTJ. AFM scanning was conducted in the inter-laced mode to ensure that topographical mapping matched with magnetic imaging.

Results and discussion: We have explored the impact of covalently bonding an array of the paramagnetic OMC molecules to the two ferromagnetic electrodes of dissimilar magnetic hardness (Fig. 1c). The MTJMSDs were studied by AFM. MTJ's topography image was recorded for monitoring structural integrity (Fig. 1d). Figure 1d is a 3D AFM image of a bare MTJ, before treating it with OMC. The reason for utilizing 3D AFM image is to show the location where OMC form molecular bridges between the top and bottom electrodes. Corresponding MFM image (Fig. 1e) showed the presence of two magnetic electrodes crossing each other at the junction. The MFM image of the top NiFe electrode revealed the microscopic features of the magnetic regions. Interestingly, bridging OMCs between two ferromagnets resulted in the near disappearance of the magnetic phase signal for the top NiFe electrode in the MTJ vicinity (Fig. 1f). The topography image showed the physical presence of OMC treated MTJ (Fig. 1g). This AFM image shows the physical presence of cross junction, top electrode, and the bottom electrode on the MTJ that was treated with OMCs and produced MFM image shown in Fig. 1f. The topography image also clearly showed the physical presence of NiFe leads extending out of the junction and possessed expected thickness. This image confirms that the top electrode that was not observed in the magnetic phase image in Fig. 1f is physically present in the topography image Fig.1g. Elsewhere in this

paper we reproduced and discussed similar MFM and topography study on another sample that was produced in a different batch with identical experimental conditions.

We also investigated the impact of OMCs on the unpatterned NiFe film. Interestingly, MFM of bare NiFe film before (Fig.1h) and after OMC interaction (Fig.1i) was almost identical. MFM study also showed the presence of magnetic domains (Fig.1h and i). Hence, it is apparent that OMC impacted a portion of NiFe electrode when it was used as a member of MTJMSD. OMC impacted MTJ's NiFe top electrode in the junction vicinity, where OMCs covalently bonded to two ferromagnetic electrodes (shown by the arrow in Fig.1d). It must be noted that NiFe is very stable ferromagnet against chemicals used for bridging OMCs between ferromagnets [18]. Due to its high stability NiFe was utilized as protection on other chemical etching sensitive metals like Co [18-20]. To further investigate OMC's impact the MFM was conducted on multiple OMC treated MTJs, discussed elsewhere in this paper.

We also investigated if the external magnetic field may impact the MFM response. In our prior study, we have also investigated MTJ testbed's transport under in-plane and out of the plane magnetic field before and after treating them with OMCs[15]. In a stable state, MTJMSDs did not respond magnetic field of ~300 Oe field. Due

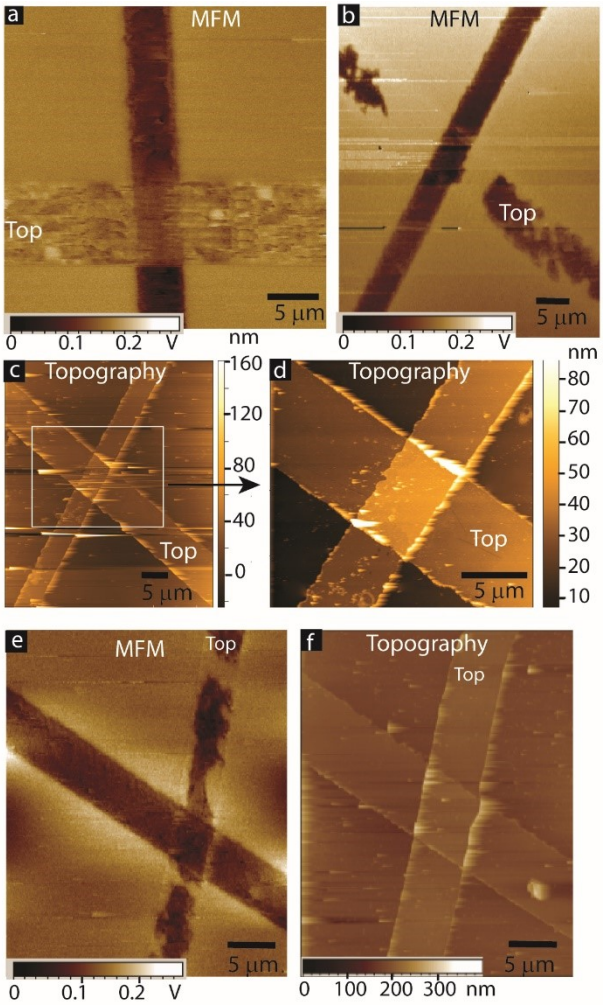

Fig. 2: MFM of MTJMSD (a) with the distinct contrast between top and bottom ferromagnets, (b) with vanished magnetic contrast near MTJ cross section, (c) AFM topography scan for the MTJMSD showing MFM in panel (b). (d) Zoomed in topography scan of the boxed area in panel (c). (e) with magnetic contrast in its transient state. (f) AFM topography corresponding to MFM image in panel (e). Panels a,b, and d adopted from ref. 13.

to that reason, we explored the magnetization by the permanent magnet to see the impact on MFM profile on MTJMSD. For this study, we subjected an MTJMSD to ~0.1 T inplane magnetic field with the help of the permanent magnet. On this MTJMSD magnetic signal did not disappear; instead, the color contrast became very distinct (Fig. 2a). Top NiFe tended to become light in color and was closer to the background color of the nonmagnetic insulating substrate. However, the bottom electrode assumed a dark color (Fig. 2a). The top and the bottom electrode are becoming radically different (Fig. 2a), but in the bare state both electrodes exhibited similar color (Fig. 1g). The top NiFe electrode also had various yellow-white color pockets. We presume these pockets as the evidence of the evolution of new magnetic phases after making OMCs connection with the ferromagnetic electrodes.

In no other circumstances, such a dramatic contrast in MFM images of an MTJ was observed. For the MTJMMSD in Fig 2a, the presence of top and bottom electrode is easily identifiable via the MFM contrast. The physical dimension of the MFM scan commensurate with topography scan collected from the adjacent MTJMSD sample discussed in Fig. 2b-d. However, in instances where MFM contrast of a ferromagnetic electrode disappear we also evaluated the MTJMSD topography. It was also noted that an MTJMSD's top magnetic electrode kept changing with time and reached a state when the magnetic phase contrast near cross junction was almost unobservable. On another sample fabricated a stable disappearance of magnetic contrast on NiFe top electrode was observed after incubating the sample for >48 hours to reach its equilibrium state after the magnetization (Fig. 2b). We also measured the topography of the MTJMSD (Fig. 2c) corresponding to the MFM scan in shown in Fig. 2b. To further ascertain that MTJMSD was indeed in stable state we performed topography scan over the boxed region shown in Fig.2c and observed presence of top electrode (Fig. 2d). Interestingly, the neighboring junction on the same sample showed the partial development of the OMC induced phases (Fig. 2e). In addition to MFM scan (Fig.2e), we also recorded the corresponding topography scan on the same junction (Fig. 2f). All the four MTJMSD samples discussed in Fig.1 -2 were physically intact.

These four MTJMSDs discussed in Fig 1-2, also clearly evidenced that ~10,000 OMCs bridges on an MTJ impacted the large area of the magnetic leads at room temperature. The estimation of the number of OMC/ tunnel junction has been discussed elsewhere [5]. We estimated the number of OMC bridges at an MTJ of 25 μm^2 junction area, possessing two exposed edges of 5 μm width. Hence, effective junction length where OMC will form bridges is 2x5 μm=10 μm. According to OMC crystallographic data, the OMC core is 1 nm wide [5, 16, 21]. If OMC assembled along the MTJ edges in the close-packed fashion, then OMC per MTJ will be 10 μm (total length of the exposed side of MTJ) divided by 1 nm (OMC width) = 10,000. This estimation is for the ideal case. However, it is expected that the order of several thousand OMCs formed the transport and spin channels between two ferromagnets of tens of micron areas. Attached number of the OMC bridges were enough to bring about a macroscopic impact shown in the MFM scans. We also discussed OMC impact on pillar form MTJs in our previous study [6]. Ashwell et al. [22] has also estimated the molecular channels along the tunnel junction edges and found the number of molecular channels in the range of several thousand.

In the present case it is apparent that several thousand OMCs are impacting microscopic MTJMSD and neighboring regions of the ferromagnetic electrodes containing billions of atoms. It is extremely challenging, to perform full scale first principle calculations to understand the OMC interaction with ferromagnetic electrodes leading to the long-range impact. Due to that we are unable to provide exact mechanism behind the OMC long range time dependent effect on microscopic magnetic tunnel junctions. Despite that, based on our past efforts we do understand that one can define the basic physics of the OMC impact on MTJMSD by the equation 1.

$$E = -J_T\left(\sum_{i\in T}\vec{S_i}\vec{S_{i+1}}\right) - J_B\left(\sum_{i\in B}\vec{S_i}\vec{S_{i+1}}\right) - J_{molT}\left(\sum_{i\in T, i+1\in mol}\vec{S_i}\vec{S_{i+1}}\right) - J_{molB}\left(\sum_{i-1\in mol, i\in B}\vec{S_{i-1}}\vec{S_i}\right) \qquad (Eq.1)$$

In eq.1 S represents the spin vector of individual atoms of ferromagnetic electrodes and molecules. In the eq. 1, J_T, and J_B, are the Heisenberg exchange coupling strengths for the top and bottom ferromagnetic

electrodes, respectively. The role of J_T, and J_B is to propagate the effect of OMC's induced exchange coupling from the tunnel junction edges to interior parts of the ferromagnetic electrodes near the junction. Each OMC molecule simultaneously connected top and bottom ferromagnetic electrodes as per the schematic is shown in Fig. 1b and the atomistic model discussed elsewhere[6]. The strength of OMC exchange coupling with the top and bottom electrode along the junction perimeter are governed by exchange coupling factors. J_{molT}, is the Heisenberg exchange coupling strengths between the top ferromagnetic electrode and OMC paramagnetic molecule. Whereas, J_{molB}, is the Heisenberg exchange coupling strength between the bottom ferromagnetic electrode and OMC paramagnetic molecule. Equation 1 only provide essential energy terms to initiate strong molecule induced exchange coupling strength and propagate in the neighboring area. We have effectively utilized the Eq. 1 to explain the experimental MFM studies on pillar form MTJMSD. Previously, OMCs produced the disappearance of MFM contrast on an array of 7000 pillar or disc shaped MTJMSDs [6], These MTJs were only designed to conduct magnetic studies by avoiding the role of ferromagnetic leads connected to the junction. Details about fabrication process and three magnetic measurements including MFM experiment are mentioned elsewhere [6]. We successfully performed Monte Carlo simulations to explain the basic science and underlying mechanism behind the microscopic MFM response on MTJMSDs. We observed that an OMC established opposite exchange coupling with the two ferromagnetic electrodes, i.e., J_{molT}, and J_{molB} were of opposite sign and were significantly strong with regards to the inter-atomic exchange coupling energy within the ferromagnetic electrode. In that case, OMC impact penetrated towards the interior part of the ferromagnetic electrodes. Typically, we reduced the number of atoms per MTJMSD to reduce the amount of time required for establishing an equilibrium state for calculating magnetic properties [6].

We assume that the basic science of MFM studies discussed in this paper is expected to be similar to simulation approach discussed in our prior work[6]. However, to study MTJMSD with extended ferromagnetic electrodes it will be essential to include a number of OMC and magnetic electrode aspects to make MC simulations meaningful and informative: (i) MC simulations need to be performed on

MTJMSD's Ising model analog with full size or much higher number of atoms, incorporating of the order of millions of atoms, to estimate realistic time for establishing equilibrium and then simulate MFM phases. (ii) MC simulations need to incorporate anisotropy energy for the ferromagnetic electrodes. In actual experiment, the top and bottom electrode had different magnetic hysteresis properties [6]. (iii) In addition, Ising model for MTJMSD's need to incorporate previously omitted biquadratic coupling and dipolar couplings to understand the propagation of OMC impact on magnetic phases on the top and bottom electrodes. However, full-fledged Monte Carlo simulations on experimentally studied cross

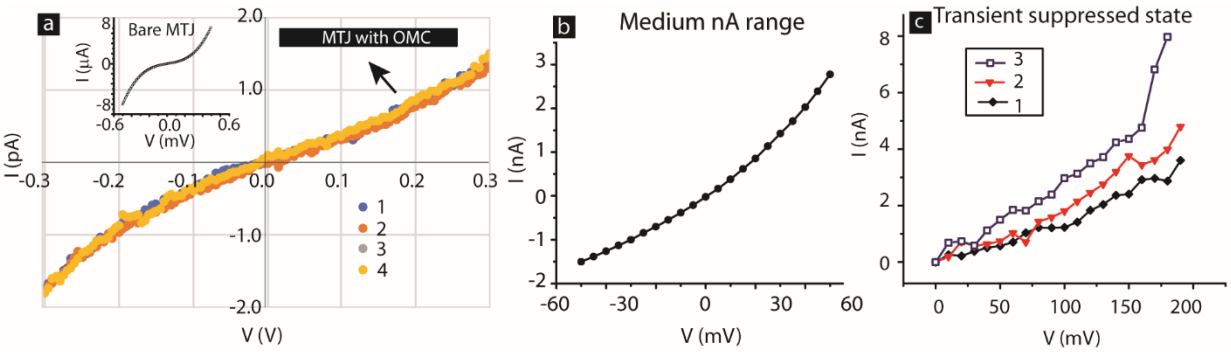

Fig. 3: (a) Current-voltage (I-V) of MTJMSD corresponding to MFM shown in panel Fig.2 (a). Inset I-V graph for MTJ before interacting with OMCs. (b) I-V of MTJMSD corresponding to MFM shown in panel Fig.2 b. (c) I-V of MTJMSD corresponding transient MFM shown in panel Fig.2e.

junction form MTJMSD (Fig.1 and 2) is beyond the scope of current paper. Pursuing MC simulations of MTJMSD may require developing a dedicated simulation program and high capacity computational machine and may be pursued as a future work.

One can obtain additional insights about the OMCs' impact on ferromagnetic electrodes that are not obvious from the above discussed Monte Carlo simulation approach. For this objective, we also studied the impact of OMC induced magnetic ordering and strong exchange coupling on the MTJMSD's transport. We observed that an MTJ, which showed a typical non-linear tunneling transport before interacting with OMC (Fig. 3a inset), settled in the suppressed current state after an incubation period. An MTJMSD appeared in a suppressed current state below MTJ's leakage current level by as much as seven orders of magnitude (Fig. 3a). The several orders of current reduction are presumably associated with the dramatic change in the ferromagnetic leads in the junction vicinity. The suppressed current state in the pA

range was observed when MTJMSD was exhibiting a significant difference in phase contrast for the top and bottom ferromagnetic electrode (Fig. 2a). The current-voltage response was in nA level (Fig. 3b) for the MFM response shown in Fig. 2b. We also observed that the current-voltage response was quite transient (Fig. 3c). We assume that this transient current-voltage behavior could be justified based on the transient MFM response near MTJMSD junction (Fig. 2c). Extensive details about OMC induced current suppression has been published elsewhere [14, 15].

In addition to exchange coupling energy-based equation (Eq.1), we also analyzed transport data before and after the OMC treatment to gain additional insights. Our hypothesis about the mechanism behind OMC impact away from the junctions are depicted in Fig. 4. An OMC molecule, containing thiol terminated long tethers [16, 17], is expected to make strong and reproducible covalent bonding with the NiFe surface atoms (Fig. 4a)[5, 18]. We have shown that our MTJMSD fabrication approach enables NiFe to form air stable Ni-S bonds [18], which are presumably stronger than the Ni-O bonds. Transport between two ferromagnetic electrodes of an as produced MTJMSD is to be determined by the cumulative energy barrier properties due to AlOx tunneling barrier and molecular channel. According to our prior study on molecular devices with non-magnetic tunnel junctions [5, 19], the transport via OMC is dominated by the tunneling through ~1 nm tether (Fig. 4a). However, in the case of MTJMSD where ferromagnetic NiFe is in direct contact with OMCs (Fig. 4a) a spin filtering action occurs via molecule core (Fig. 4c). Due to this

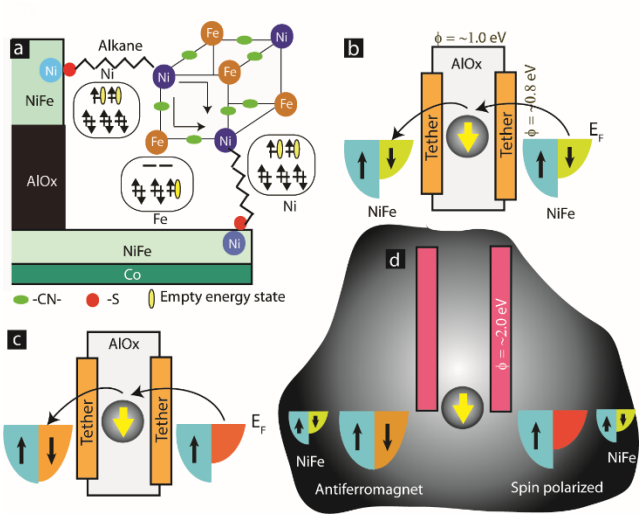

Fig. 4: Hypothetical Mechanism. (a) OMC connected to NiFe film of top and bottom ferromagnets of an MTJ, (b) representative energy barriers of AlOx and OMC between NiFe top and bottom ferromagnet. (c) molecule induced spin filtering impacting the spin density close to molecular junction, (d) molecule impacted density of state of the top and bottom ferromagnet establish equilibrium with macroscopic ferromagnets away from the junction area.

spin filtering effect, the spin density of states of the ferromagnetic electrodes is strongly altered in the vicinity of molecular junction (Fig. 4c). Fig.4c shows the OMC promoted the movement of spin down electrons on to the top NiFe ferromagnet. It is hypothesized that an OMC, which possesses Ni and Fe atoms with a vacancy for one type of spin, will only allow selective spin transport (Fig. 4a). For instance, spin down (or spin up) electrons from the bottom electrode may keep moving to the spin-down band of the top ferromagnetic electrode (Fig. 4b). As a result, the bottom ferromagnetic electrode may be depleted with the spin down (or spin up) electron spin density to become more spin polarized and getting higher contrast (Fig. 4c). However, the top ferromagnet may become equal in spin up and spin down electron population near the junction area (Fig. 4c-d). In this state, NiFe ferromagnet may appear as quasi anti-ferromagnet near the molecular junction that appears as a region without discernible magnetic phase or disappears in the MFM. Resultantly, top NiFe may end up becoming non-ferromagnetic while bottom NiFe may become highly spin-polarized (Fig. 4c).

Also, the energy barrier height is a function of the density of states of the metallic electrodes on either side of the tunnel junctions [4]. Hence, an MTJMSD is expected to attain remarkably different magnetic properties of the ferromagnetic electrodes and barrier properties (Fig. 4d). In our two prior publications, we have analyzed the barrier properties of an MTJMSD in the suppressed current state[14, 15]. We estimated the effective barrier heights and barrier thicknesses using Brinkman tunneling models [23]. A bare MTJ exhibited ~2.2 nm barrier thickness and ~0.7 eV barrier height (Fig. 3a). After hosting OMC channels along the exposed side edges, an MTJ became MTJMSD and showed very different barrier properties in the pA range suppressed current state (Fig. 3a). According to modeling results in the suppressed current state OMC treated MTJ, or MTJMSD exhibited ~1.4 nm barrier thickness and ~ 2.2 eV barrier heights. Importantly the barrier thickness after hosting OMCs is equivalent to the length of a decane molecule chain that connected the core of OMC molecules to the NiFe electrode in an MTJMSD (Fig. 4a). Hence, OMCs' transformative impact is evident from the transport and MFM studies both. In

our prior study, we discussed the OMC role in producing unprecedented spin filtering leading to dramatic change in ferromagnetic electrodes degree of spin polarization[15]

MFM response on MTJMSD depends on the magnetic properties of the OMC impacted ferromagnetic electrodes. In this paper, we mainly discuss the OMC impact on spin polarization [15]. The magnetic properties of ferromagnets depend on the density of state of the spin up and spin down electrons [24]. We surmise that under the influence of molecular coupling, a new effective electrode evolves due to the hybridization of molecular energy levels with the spin density of states of the original ferromagnetic electrodes (before introducing OMCs). After strong hybridization, a discreet molecular energy level is expected to broaden [25]. However, the molecular energy levels are degenerate for spin up and spin down electrons. The effective density of states of the major and minority spin density of states in a molecule affected ferromagnetic electrode is a result of molecule mediated spin filtering [25]. Molecule spin state is expected to play a crucial role in spin filtering [26]. The OMC molecule is capable of attaining the S=6 spin state in the isolated state [16, 17]. We presumed that this S=6 state is still applicable when an OMC is bonded to the ferromagnetic electrodes. In this state, it seems that iron (Fe) and Ni atoms of the OMC clusters are open for accommodating only one specific type of spin due to selection rule [27]. Several thousands of OMCs are connected to two ferromagnetic electrodes via alkane barrier and thiol chemical bonding. Thiol group has been utilized to bond OMC to the ferromagnet. It is noteworthy that simple thiol functionalization of even nonmagnetic gold metal electrode has produced magnetism [28]. We expect that such OMC induced spin filtering would continue until the spin density of states on two electrodes reaches a new equilibrium. Also, OMC impact is expected to influence a limited range of the ferromagnet due to the reason mentioned with regards to equation 1. Hence, part of the top and bottom ferromagnetic electrodes away from the junction are expected to be unaffected. Depending on the magnetic anisotropy, physical dimensions, and magnetic molecules, the impact of molecule induced exchange coupling may be different on top and bottom ferromagnetic electrodes. For instance, in MTJMSDs mainly top NiFe electrode's MFM response underwent significant change. Our primary hypothesis is by no means complete. There are various

other possibilities in the manner OMC may impact ferromagnetic leads near the junction. Future experimental and theoretical studies are expected to provide accurate and more profound insights about the OMCs' impact.

Conclusions: This paper discussed the experimental magnetic force microscopy (MFM) studies on MTJMSDs. We showed that molecules are much more than simple spin channels between two magnetic electrodes. MFM produced vivid evidence showing that a paramagnetic molecule covalently bonded to the two ferromagnetic electrodes catalyzed a large-scale ordering on ferromagnetic electrodes and impacted several hundred-micron areas near molecular junctions. Transport studies showed that paramagnetic molecule induced long-range impact on ferromagnetic electrodes resulted in several orders of current suppression at room temperature. Future studies about molecule impact on various forms of magnetic tunnel junctions are in order.

Acknowledgments: Pawan Tyagi thanks Dr. Bruce Hinds and Department of Chemical and Materials engineering at University of Kentucky for facilitating experimental work on MTJMSD during his PhD. PT thanks Dr. Stephen Holmes and his postdoctoral scholar Dr. D.F. Li for producing OMC. The preparation of this paper was in part supported by National Science Foundation-CREST Award (Contract # HRD-1914751), Department of Energy/ National Nuclear Security Agency (DE-NA0003945), and Air Force Office of Sponsored Research (Award #FA9550-13-1-0152). Any opinions, findings, and conclusions expressed in this paper are those of the author(s) and do not necessarily reflect the views of any funding agency and corresponding author's past and present affiliations.

References:

[1] L. Bogani and W. Wernsdorfer, "Molecular spintronics using single-molecule magnets," *Nat. Mater.,* vol. 7, pp. 179-186, Mar 2008.

[2] S. Sanvito, "Injecting and controlling spins in organic materials," *J. Mater. Chem.,* vol. 17, pp. 4455-4459, 2007.

[3] N. Prokopuk and K. A. Son, "Alligator clips to molecular dimensions," *J. Phys.-Condes. Matter,* vol. 20, p. 374116, Sep 17 2008.

[4] G. X. Miao, M. Munzenberg, and J. S. Moodera, "Tunneling path toward spintronics," *Rep. Prog. Phys.,* vol. 74, p. 036501, 2011.

[5] P. Tyagi, D. F. Li, S. M. Holmes, and B. J. Hinds, "Molecular Electrodes At The Exposed Edge Of Metal/Insulator/Metal Trilayer Structures," *J. Am. Chem. Soc.,* vol. 129, pp. 4929-4938, Apr 25 2007.

[6] P. Tyagi, C. Baker, and C. D'Angelo, "Paramagnetic Molecule Induced Strong Antiferromagnetic Exchange Coupling on a Magnetic Tunnel Junction Based Molecular Spintronics Device," *Nanotechnology,* vol. 26, p. 305602, 2015.

[7] A. N. Pasupathy, R. C. Bialczak, J. Martinek, J. E. Grose, L. A. K. Donev, P. L. McEuen*, et al.*, "The Kondo effect in the presence of ferromagnetism," *Science,* vol. 306, pp. 86-89, Oct 1 2004.

[8] J. R. Heath, "Molecular electronics," *Annual Review of Materials Research,* vol. 39, pp. 1-23, 2009.

[9] A. J. Epstein, "Organic-based magnets: Opportunities in photoinduced magnetism, spintronics, fractal magnetism, and beyond," *MRS Bull.,* vol. 28, pp. 492-499, Jul 2003.

[10] J. R. Petta, S. K. Slater, and D. C. Ralph, "Spin-dependent transport in molecular tunnel junctions," *Phys. Rev. Lett.,* vol. 93, p. 136601, Sep 24 2004.

[11] P. Tyagi, "Multilayer Edge Molecular Electronics Devices: A Review," *J. Mater. Chem.,* vol. 21, pp. 4733-4742, 2011.

[12] Y. Fujisaki, "Review of emerging new solid-state non-volatile memories," *Jpn. J. Appl. Phys.,* vol. 52, p. 040001, 2013.

[13] P. Tyagi and C. Riso, "Photovoltaic Effect on Molecule Coupled Ferromagnetic Films of a Magnetic Tunnel Junction " *arXiv:1112.1879 [cond-mat.mes-hall],* p. , 2019.

[14] P. Tyagi and E. Friebe, "Large Resistance Change on Magnetic Tunnel Junction based Molecular Spintronics Devices," *J. Mag. Mag. Mat.,* vol. 453, pp. 186-192, 2018.

[15] P. Tyagi, C. Riso, and E. Friebe, "Magnetic Tunnel Junction Based Molecular Spintronics Devices Exhibiting Current Suppression At Room Temperature," *Organic Electronics,* vol. 64, pp. 188-194, 2019.

[16] D. F. Li, S. Parkin, G. B. Wang, G. T. Yee, R. Clerac, W. Wernsdorfer*, et al.*, "An S=6 cyanide-bridged octanuclear (Fe4Ni4II)-Ni-III complex that exhibits slow relaxation of the magnetization," *J. Am. Chem. Soc.,* vol. 128, pp. 4214-4215, Apr 5 2006.

[17] D. F. Li, C. Ruschman, R. Clerac, and S. M. Holmes, "Ancillary Ligand Functionalization of Cyanide-Bridged S = 6 FeIII4NiII4 Complexes for Molecule-Based Electronics," *Inorg. Chem.,* vol. 45, p. 7569, 2006.

[18] P. Tyagi, E. Friebe, and C. Baker, "Addressing The Challenges Of Using Ferromagnetic Electrodes In The Magnetic Tunnel Junction-Based Molecular Spintronics Devices," *J.Nanoparticle Res.,* vol. 17, p. 452, Nov 2015.

[19] P. Tyagi, "Fabrication of Tunnel Junction based Molecular Electronics and Spintronics Devices " *J. Nanoparticle Res.,* vol. 14, p. 1195, 2012.

[20] P. Tyagi and B. J. Hinds, "Mechanism of Ultrathin Tunnel Barrier Failure Due to Mechanical Stress Induced Nano-Sized Hillocks and Voids," *J. Vac. Sci. Technol. B,* vol. 28, pp. 517-521, 2010.

[21] D. Li, R. Clérac, O. Roubeau, E. Harté, C. Mathonière, R. Le Bris*, et al.*, "Magnetic and Optical Bistability Driven by Thermally and Photoinduced Intramolecular Electron Transfer in a Molecular Cobalt−Iron Prussian Blue Analogue," *J. Am. Chem. Soc.,* vol. 130, pp. 252-258, 2008/01/01 2008.

[22] G. J. Ashwell, P. Wierzchowiec, C. J. Bartlett, and P. D. Buckle, "Molecular electronics: connection across nano-sized electrode gaps," *Chem. Commun.,* pp. 1254-1256, 2007.

[23] W. F. Brinkman, R. C. Dynes, and J. M. Rowell, "Tunneling Conductance of Asymmetrical Barriers," *J. Appl. Phys.,* vol. 41, p. 1915, 1970.

[24] J. M. Coey, *Magnetism and magnetic materials*: Cambridge University Press, 2010.

[25] M. Galbiati, *Molecular Spintronics : From Organic Semiconductors to Self-Assembled Monolayers*. Switzerland: Springer International Publishing, 2015.

[26] P. N. Abufager, R. Robles, and N. Lorente, "FeCoCp3 Molecular Magnets as Spin Filters," *J. Phys. Chem. C,* vol. 119, pp. 12119-12129, Jun 2015.

[27] H. B. Heersche, Z. de Groot, J. A. Folk, H. S. J. van der Zant, C. Romeike, M. R. Wegewijs*, et al.*, "Electron transport through single Mn-12 molecular magnets," *Phys. Rev. Lett.,* vol. 96, p. 206801, May 26 2006.

[28] P. Crespo, R. Litran, T. C. Rojas, M. Multigner, J. M. de la Fuente, J. C. Sanchez-Lopez*, et al.*, "Permanent magnetism, magnetic anisotropy, and hysteresis of thiol-capped gold nanoparticles," *Phys. Rev. Lett.,* vol. 93, p. 087204, Aug 20 2004.